ChemComm

This article is part of the

Porphyrins & Phthalocyanines

web themed issue

Guest editors: Jonathan Sessler, Penny Brothers and Chang-Hee Lee

All articles in this issue will be gathered together online at
www.rsc.org/porphyrins

ChemComm

Dynamic Article Links

Cite this: *Chem. Commun.*, 2012, **48**, 4368–4370

www.rsc.org/chemcomm

COMMUNICATION

Design and characterization of alkoxy-wrapped push–pull porphyrins for dye-sensitized solar cells†‡

Teresa Ripolles-Sanchis,[a] Bo-Cheng Guo,[b] Hui-Ping Wu,[c] Tsung-Yu Pan,[c] Hsuan-Wei Lee,[b] Sonia R. Raga,[a] Francisco Fabregat-Santiago,[a] Juan Bisquert,*[a] Chen-Yu Yeh*[b] and Eric Wei-Guang Diau*[c]

Received 15th February 2012, Accepted 9th March 2012
DOI: 10.1039/c2cc31111a

Three alkoxy-wrapped push–pull porphyrins were designed and synthesized for dye-sensitized solar cell (DSSC) applications. Spectral, electrochemical, photovoltaic and electrochemical impedance spectroscopy properties of these porphyrin sensitizers were well investigated to provide evidence for the molecular design.

Porphyrins are promising candidates as highly efficient sensitizers for dye-sensitized solar cells (DSSC) because of their superior light-harvesting ability in the visible region.[1–3] Recent advances on the development of a porphyrin sensitizer (**YD2-*o*-C8**) with co-sensitization of an organic dye (**Y123**) using a cobalt-based electrolyte attained a power conversion efficiency of 12.3%,[4] which is superior to those developed based on Ru complexes[5] and becomes a new milestone in this area. The key structural feature on molecular design of a highly efficient porphyrin sensitizer is to bear with long alkoxyl chains in the *ortho*-positions of the *meso*-phenyls so as to effectively envelope the porphyrin ring to reduce the degree of dye aggregation for a higher electron injection yield and to form a blocking layer for a better charge collection yield.[6] In the present study, we further design three porphyrin sensitizers (**YD20–YD22**, Chart 1) based on the structure of **YD2-*o*-C8** but with extended π-conjugation in order to enhance the light-harvesting ability. Basically all of them have the same *ortho*-substituted porphyrin core with two phenylethynyl (PE) groups acting as a π-bridge in the *meso*-position of the ring. **YD20** and **YD22** dyes have the acceptor group (ethynylbenzoic acid) the same as that of **YD2-*o*-C8** but with different donor groups: **YD20** has a triphenylamino group with two methoxyl substitutes and **YD22** has a phenylamino group with two *n*-butyl chains. On the other hand, **YD20** and **YD21** dyes have the same donor group but the cyanoacrylic acid was used as an anchoring group in **YD21**. This approach mimics the molecular design of an organic dye[7] having the acrylonitrile group with strong electron-pulling power to act as an efficient acceptor for the porphyrin dye.

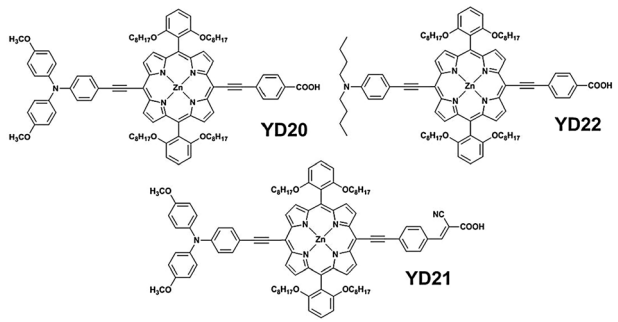

Chart 1 Molecular structures for **YD20–YD22** porphyrin dyes.

The details for the syntheses, optical and electrochemical characterizations of **YD20–YD22** are given in ESI.‡ These porphyrin dyes were fabricated into DSSC devices for photovoltaic and electrochemical impedance spectroscopy (EIS) characterizations. Fig. 1a and b show the *J–V* curves and the corresponding Incident Photon to Current Conversion Efficiency (IPCE) action spectra for the **YD20–YD22** devices, respectively; the obtained photovoltaic parameters and the amounts of dye-loading are summarized in Table 1. The results indicate that the short-circuit current densities (J_{SC}) exhibit a trend **YD20** > **YD22** > **YD21** and the open-circuit voltages (V_{OC}) display a trend **YD20** > **YD22** ~ **YD21**; the overall power conversion efficiencies (η) show the same order as J_{SC}, which is consistent with the variations of the IPCE action spectra showing the same order. As a result, **YD20** has the highest J_{SC} (17.43 mA cm^{-2}) and V_{OC} (676 mV), which yields the greatest η (8.1%) among the three porphyrins under investigation. Even though the cyanoacrylic substitute makes **YD21** a slight red shift in the absorption spectrum (Fig. S1, ESI‡), the floppy feature of the C=C double bond might tilt the molecules adsorbed on TiO_2 film to significantly decrease its IPCE values and the corresponding current density. However, **YD20** and **YD22** have the same anchoring group and very similar

[a] *Photovoltaics and Optoelectronic Devices Group, Departament de Física, Universitat Jaume I, 12071 Castelló, Spain. E-mail: bisquert@fca.uji.es; Tel: +34-964-38-7540*
[b] *Department of Chemistry and Center of Nanoscience & Nanotechnology, National Chung Hsing University, Taichung 402, Taiwan. E-mail: cyyeh@dragon.nchu.edu.tw; Fax: +886-4-22862547; Tel: +886-4-22852264*
[c] *Department of Applied Chemistry and Institute of Molecular Science, National Chiao Tung University, Hsinchu 30010, Taiwan. E-mail: diau@mail.nctu.edu.tw; Fax: +886-3-5723764; Tel: +886-3-5131524*

† This article is part of the ChemComm "Porphyrins and Phthalocyanines" web themed issue.

‡ Electronic supplementary information (ESI) available. See DOI: 10.1039/c2cc31111a

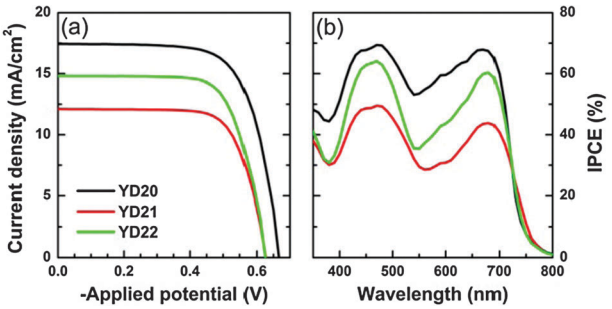

Fig. 1 (a) Current *vs.* voltage characteristics of DSSC devices prepared with YD20 (black), YD21 (red), and YD22 (green) under illumination of simulated AM 1.5 full sunlight (100 W cm^{-2}) with an active layer of 0.16 cm^2 and (b) the corresponding action spectra for the efficiency of incident photon-to-current conversion (IPCE).

Table 1 Photovoltaic parameters of porphyrin-based dye-sensitized solar cells (active layer 0.16 cm^2) under 100 mW cm^{-2} light illumination (AM 1.5 G) for **YD20–YD22**

Dye	Dye loading/ nmol cm^{-2}	J_{SC}/ mA cm^{-2}	V_{OC}/ mV	FF	η (%)
YD20	161	17.43	676	0.686	8.1
YD21	132	12.05	631	0.721	5.5
YD22	134	14.87	634	0.700	6.6

absorption spectra (Fig. S1, ESI‡), therefore, the differences in IPCE and photocurrent are related to the effect of the donor groups. Note that the decrease in the IPCE occurs at a nearly constant level for all the wavelengths of the spectra for **YD21** compared to **YD20**. Thus, the loss of electrons is independent of the energy of the absorbed photons. Transport and injection losses may be considered for the decrease in IPCE, which is discussed in the following.

Dye loading measurements yielded 161, 132, and 134 nmol cm^{-2} for **YD20**, **YD21** and **YD22**, respectively. The changes in J_{SC} between the dyes with the same anchoring group, **YD20** and **YD22**, may be understood in terms of the different amounts of loaded sensitizer. Further explanation is needed for sample **YD21** as the decrease in J_{SC} is larger despite the amount of dye loading in the cell is the same as for **YD22**.

Electrochemical Impedance Spectroscopy was used to complete the analysis of injection and to gain insight into the transport and charge losses characteristics of the DSSC with the different dyes.[8] From the fitting of impedance spectra of the DSSC at different applied potentials under 1 sun illumination, we obtained the chemical capacitance (C_μ), transport resistance in the TiO_2 (R_{tr}), recombination resistance (R_{rec}), as a function of the Fermi level voltage (V_F) shown in Fig. 2a, b, and c, respectively. Other contributions to the total resistance of the cell such as diffusion, counter electrode and FTO resistances were grouped as series resistance (R_s). The effect of R_s in the applied potential (V_{app}) was removed to obtain the V_F that may be calculated through $V_F = V_{app} - jR_s$. From the plot of C_μ *vs.* $-V_F$ shown in Fig. 2a, the position of the conduction band edge of TiO_2 (E_c) may be estimated as reported elsewhere.[9] Through these calculations, we estimated that for **YD20** $E_c \approx -0.48$ V *vs.* NHE, while for **YD21** E_c was displaced +4 mV and **YD22** −10 mV. Data from transport resistance shown in Fig. 2b also provide very small displacements in E_c, corroborating that

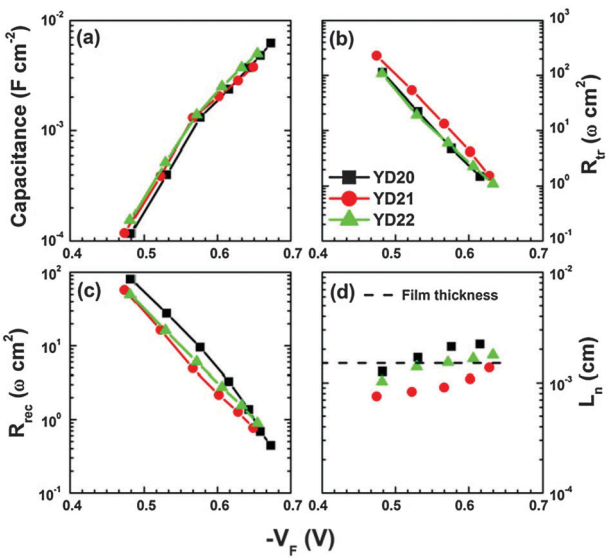

Fig. 2 (a) Capacitance, (b) transport resistance, (c) recombination resistance, and (d) diffusion length of **YD20–YD22** dyes in DSSC plotted with respect to the Fermi level voltage ($-V_F$) with removing the effect of series resistance.

all the TiO_2 conduction bands remain almost unchanged for the three dyes as obtained from the capacitance data.

To understand the origin of the small differences in the V_{OC} found for the three different dyes it is needed to analyze the behavior of the recombination resistance in Fig. 2c. In previous studies,[8,10] when comparing the recombination resistance of different samples it has been found that the higher the value of R_{rec}, the larger the V_{OC}, while only very large changes in photocurrent produce small variations in V_{OC}. The results here match very well with this analysis: as it can be seen in Fig. 2c, **YD20** has the larger recombination resistance and V_{OC}, whereas **YD21** and **YD22** have similar values of R_{rec} showing almost the same V_{OC}.

Data from R_{rec} and R_{tr} may be used to calculate the diffusion length (L_n) in TiO_2 film shown in Fig. 2d as[8]

$$L_n = L\sqrt{R_{rec}/R_{tr}} \quad (1)$$

where L is the film thickness (15 μm) represented as a dashed curve in Fig. 2d. The L_n values exhibit a systematic trend with the order **YD20** > **YD22** > **YD21** with those of **YD20** and **YD22** reaching values greater than their film thickness whereas those of **YD21** being significantly smaller than the film thickness. This implies that the **YD21** device suffers from a poorer collection efficiency of injected electrons what produces the extra decrease in J_{SC} found for this sample.

The small differences found for the position of the conduction band edge (E_c) may also help to fine tune the roles of the linker in these Zn–porphyrin dyes. If the Fermi level potential is shifted the amounts found for the displacement of E_c, it is possible to compare the recombination resistance of the DSSC at the potential level with the same number of injected electrons. To do this we define the potential at the equivalent conduction band position[8]

$$V_{ecb} = V_F - \Delta E_c/e \quad (2)$$

where e is the electron charge and $\Delta E_c = E_c - E_{c,ref}$, for which $E_{c,ref}$ is the position of the conduction band of **YD20**. Based on

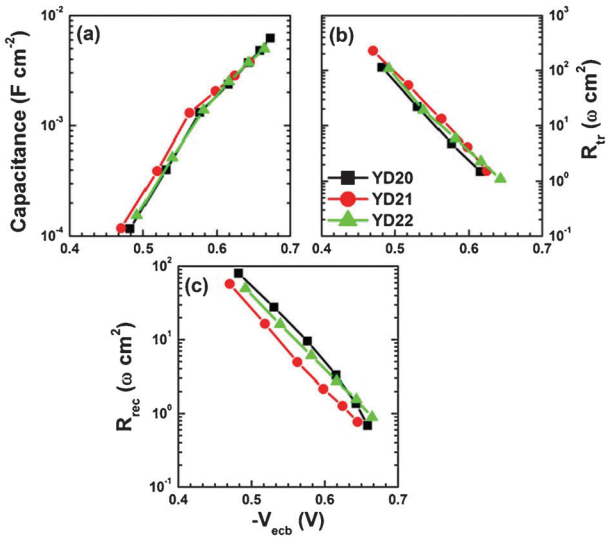

Fig. 3 (a) Capacitance, (b) transport resistance, and (c) recombination resistance of **YD20–YD22** dyes in DSSC plotted with respect to the equivalent common conduction band voltage ($-V_{ecb}$).

these conditions, we transfer Fig. 2a–c into Fig. 3a–c, which show C_μ (a), R_{tr} (b), and R_{rec} (c) as a function of $-V_{ecb}$. While the chemical capacitance (Fig. 3a) and the transport resistance (Fig. 3b) of the three dyes match quite well, the recombination resistance (Fig. 3c) of the **YD21** device is much smaller compared to that of the **YD20** and **YD22** devices. In other words, charge recombination is a major problem for the poor performance of the **YD21** device. These results allow us to make a conclusion: compared to the **YD20** device, the smaller V_{OC} of **YD22** was due to a small shift in conduction band but the smaller V_{OC} of **YD21** was due to a significant charge recombination. From the structural viewpoint, the use of cyanoacrylic acid as an acceptor and an anchoring group in **YD21** might provide more free space (less amount of dye-loading) for the charge recombination than the use of the rigid ethynylbenzoic acid in **YD20** and **YD22**. Moreover, **YD21** might be tilted on the surface of TiO_2 for the charge recombination to occur more easily.

In conclusion, although the concept for molecular design with the cyanoacrylic acid acceptor has been widely applied in highly efficient organic dyes,[7] such an approach does not work well for the porphyrin sensitizers as demonstrated herein. The greater performance in the **YD20** device than the other two devices is attributed to its rigid structural feature for a larger amount of dye-loading, which combined with the higher recombination resistance and diffusion length yields to larger J_{SC} and V_{OC}. Modification of the porphyrin structure with extended π-conjugation for better light harvesting is feasible to boost up the device performance in the near future.

This work was partially supported by National Science Council of Taiwan and Ministry of Education of Taiwan, under the ATU program. JB acknowledges support by projects from Ministerio de Ciencia e Innovación (MICINN) of Spain (Consolider HOPE CSD2007-00007, MAT2010-19827), and Generalitat Valenciana (PROMETEO/2009/058). SRR thanks financial support from Bancaixa foundation under project Innova 11I272. CYY and EWGD acknowledge support by projects from National Science Council of Taiwan and Ministry of Education of Taiwan, under the ATU program.

Notes and references

1 (*a*) H. Imahori, T. Umeyama and S. Ito, *Acc. Chem. Res.*, 2009, **42**, 1809–1818; (*b*) M. V. Martínez-Díaz, G. de la Torre and T. Torres, *Chem. Commun.*, 2010, **46**, 7090–7108; (*c*) X.-F. Wang and H. Tamiaki, *Energy Environ. Sci.*, 2010, **3**, 94–106.
2 (*a*) C.-W. Lee, H.-P. Lu, C.-M. Lan, Y.-L. Huang, Y.-R. Liang, W.-N. Yen, Y.-C. Liu, Y.-S. Lin, E. W.-G. Diau and C.-Y. Yeh, *Chem.–Eur. J.*, 2009, **15**, 1403–1412; (*b*) H.-P. Lu, C.-L. Mai, C.-Y. Tsia, S.-J. Hsu, C.-P. Hsieh, C.-L. Chiu, C.-Y. Yeh and E. W.-G. Diau, *Phys. Chem. Chem. Phys.*, 2009, **11**, 10270–10274; (*c*) H.-P. Lu, C.-Y. Tsai, W.-N. Yen, C.-P. Hsieh, C.-W. Lee, C.-Y. Yeh and E. W.-G. Diau, *J. Phys. Chem. C*, 2009, **113**, 20990–20997; (*d*) C.-P. Hsieh, H.-P. Lu, C.-L. Chiu, C.-W. Lee, S.-H. Chuang, C.-L. Mai, W.-N. Yen, S.-J. Hsu, E. W.-G. Diau and C.-Y. Yeh, *J. Mater. Chem.*, 2010, **20**, 1127–1134; (*e*) T. Bessho, S. M. Zakeeruddin, C.-Y. Yeh, E. W.-G. Diau and M. Grätzel, *Angew. Chem., Int. Ed.*, 2010, **49**, 6646–6649.
3 (*a*) C.-Y. Lin, C.-F. Lo, L. Luo, H.-P. Lu, C.-S. Hung and E. W.-G. Diau, *J. Phys. Chem. C*, 2009, **113**, 755–764; (*b*) C.-Y. Lin, Y.-C. Wang, S.-J. Hsu, C.-F. Lo and E. W.-G. Diau, *J. Phys. Chem. C*, 2010, **114**, 687–693; (*c*) C.-F. Lo, S.-J. Hsu, C.-L. Wang, Y.-H. Cheng, H.-P. Lu, E. W.-G. Diau and C.-Y. Lin, *J. Phys. Chem. C*, 2010, **114**, 12018–12023; (*d*) C.-L. Wang, Y.-C. Chang, C.-M. Lan, C.-F. Lo, E. W.-G. Diau and C.-Y. Lin, *Energy Environ. Sci.*, 2011, **4**, 1788–1795.
4 A. Yella, H.-W. Lee, H. N. Tsao, C. Yi, A. K. Chandiran, M. K. Nazeeruddin, E. W.-G. Diau, C.-Y. Yeh, S. M. Zakeeruddin and M. Grätzel, *Science*, 2011, **334**, 629–634.
5 (*a*) C.-Y. Chen, M. Wang, J.-Y. Li, N. Pootrakulchote, L. Alibabaei, C. Ngoc-Ie, J.-D. Decoppet, J.-H. Tsai, C. Grätzel, C.-G. Wu, S. M. Zakeeruddin and M. Grätzel, *ACS Nano*, 2009, **3**, 3103–3109; (*b*) Y. Cao, Y. Bai, Q. Yu, Y. Cheng, S. Liu, D. Shi, F. Gao and P. Wang, *J. Phys. Chem. C*, 2009, **113**, 6290–6297; (*c*) Q. Yu, Y. Wang, Z. Yi, N. Zu, J. Zhang, M. Zhang and P. Wang, *ACS Nano*, 2010, **4**, 6032–6038.
6 (*a*) Y.-C. Chang, C.-L. Wang, T.-Y. Pan, S.-H. Hong, C.-M. Lan, H.-H. Kuo, C.-F. Lo, H.-Y. Hsu, C.-Y. Lin and E. W.-G. Diau, *Chem. Commun.*, 2011, **47**, 8910–8912; (*b*) C.-L. Wang, C.-M. Lan, S.-H. Hong, Y.-F. Wang, T.-Y. Pan, C.-W. Chang, H.-H. Kuo, M.-Y. Kuo, E. W.-G. Diau and C.-Y. Lin, *Energy Environ. Sci.*, 2012, DOI: 10.1039/C2EE03308A, Advance Article.
7 (*a*) G. Zhang, H. Bala, Y. Cheng, D. Shi, X. Lv, Q. Yu and P. Wang, *Chem. Commun.*, 2009, 2198–2200; (*b*) Z. Ning and H. Tian, *Chem. Commun.*, 2009, 5483–5495; (*c*) Z. Ning, Y. Fu and H. Tian, *Energy Environ. Sci.*, 2010, **3**, 1170–1181.
8 F. Fabregat-Santiago, G. Garcia-Belmonte, I. Mora-Sero and J. Bisquert, *Phys. Chem. Chem. Phys.*, 2011, **13**, 9083–9118.
9 E. M. Barea, J. Ortiz, F. J. Payá, F. Fernández-Lázaro, F. Fabregat-Santiago, A. Sastre-Santos and J. Bisquert, *Energy Environ. Sci.*, 2010, **3**, 1985–1994.
10 (*a*) E. M. Barea, C. Zafer, B. Gultekin, B. Aydin, S. Koyuncu, S. Icli, F. F. Santiago and J. Bisquert, *J. Phys. Chem. C*, 2010, **114**, 19840–19848; (*b*) E. M. Barea, V. González-Pedro, T. Ripollés-Sanchis, H.-P. Wu, L.-L. Li, C.-Y. Yeh, E. W.-G. Diau and J. Bisquert, *J. Phys. Chem. C*, 2011, **115**, 10898–10902.

